# Bending a Colossal Magnetoresistance

*A new combination of heteroepitaxial $Pr_{0.5}Ca_{0.5}MnO_3/SrTiO_3$ grown on F-mica, shows that excellent mechanical modulation of CMR, in the range ~1000%, can be achieved at low temperature.*

Heteroepitaxial flexible oxides exhibit many interesting properties that make them strong candidates for next-generation flexible electronic devices.[1-5] Recent studies have shown that fluorophlogopite mica (F-mica, also called common mica or muscovite) is a suitable substrate for growing such heteroepitaxial oxides because of its excellent flexibility and high-temperature stability required for applications. For example, superior performance was demonstrated for transparent conductive indium tin oxide,[2] aluminium-doped ZnO,[3] ferroelectric $BaTiO_3$,[4] ferromagnetic $SrRuO_3$,[5] *etc*. grown on F-mica substrates.

Perovskite manganite $Pr_{0.5}Ca_{0.5}MnO_3$ (PCMO) in its bulk form exhibits an antiferromagnetic/charge-ordered (AFM/CO) phase that can be melted on the application of a magnetic field, but the melting field required for bulk samples is large (~27 T), impeding practical applications. A major improvement was the growth of PCMO films on $SrTiO_3$ (STO) substrates, which resulted in decreasing the melting field to 5 T. With the aim of investigating mechanical control of the properties of the PCMO/STO heteroepitaxial oxide system, researchers have now grown PCMO/STO heteroepitaxial films on F-mica.[1]

The authors used pulsed-laser deposition to grow a buffer STO layer on F-mica, followed by PCMO films on the STO, as shown schematically in **Figs. 1(a) and 1(b)**. Synchrotron-based X-ray diffraction was implemented on **TLS 13A1** and **TLS 17B1** at the NSRRC in order to characterize the crystal structure and epitaxy of the PCMO/STO films. The out-of-plane normal scan clearly showed the pristine phase of PCMO, STO and F-mica substrate with only signals in the (111) series of PCMO and STO appearing, along with (00L) signals of F-mica (**Fig. 1(c)**). Further, as shown in **Fig. 1(d)**, the omega scan of PCMO exhibited full width 0.72° at half maximum, indicating crystallinity of the PCMO layer better than in earlier work. Phi scans were also employed by the authors to study the in-plane structural quality of the films. **Figure 1(e)** shows that signals corresponding to PCMO (002), STO (002) and F-mica (202) were detected every 60°, showing well aligned six-fold symmetry, confirming the excellent heteroepitaxy. XRD reciprocal-space mapping (RSM) of PCMO (002), STO (002) and F-mica (202) signals agreed with the results from the Phi scans, indicating strain-free films of PCMO and STO layers consistent with the normal scan data.

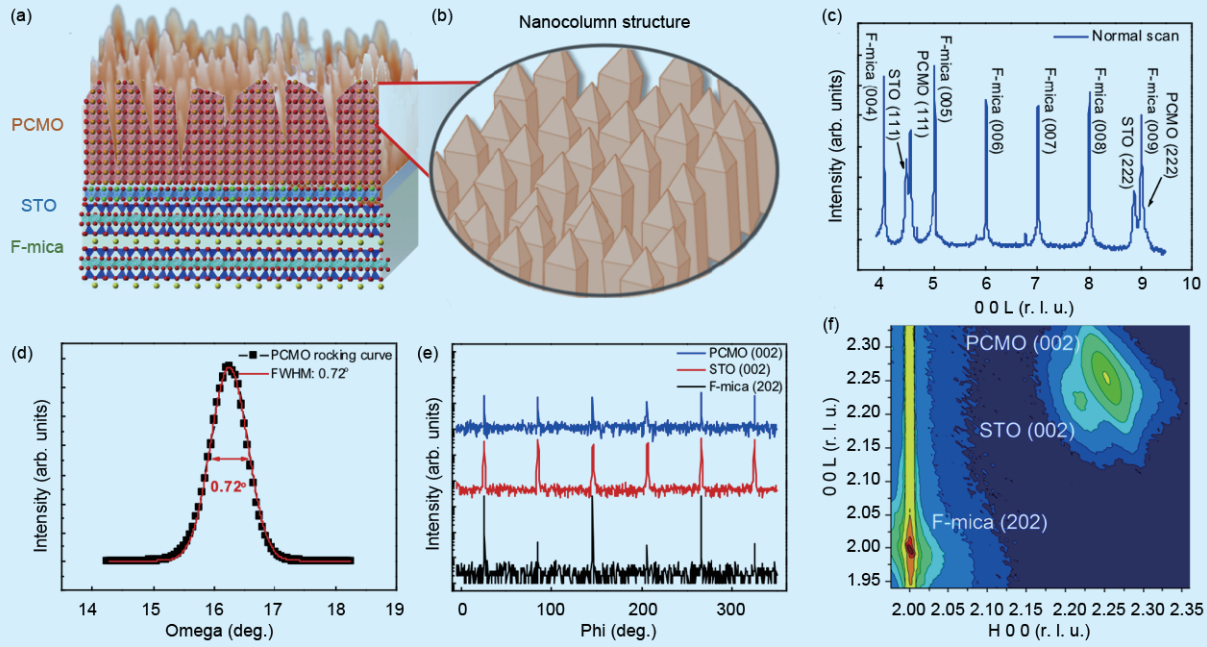


**Fig. 1**: (a) Schematic graph of epitaxial structure of PCMO/F-mica and (b) enlarged surficial region showing a nanocolumn structure. XRD analyses of PCMO/F-mica including (c) normal scan of (00L) series of F-mica with PCMO (111) and (222), (d) omega scan of PCMO (111), (e) phi scans of F-mica (202), STO (002), and PCMO (002) and (f) Reciprocal-space mapping of F-mica (202) with STO (002) and PCMO (002). [Reproduced from Ref. 1]

The authors then used X-ray absorption spectra (XAS) *in situ* at **TPS 45A1** to determine the valence state of the Pr and Mn ions in the heteroepitaxial films. **Figure 2(a)** shows the isotropic Pr $M_{4,5}$ XAS from the PCMO layer measured at 300 K with that of $Pr_2O_3$, a standard $Pr^{3+}$ reference sample. The similar spectral features of the PCMO film and $Pr_2O_3$ indicate that Pr ions in the PCMO layer are trivalent. **Figure 2(b)** shows the isotropic Mn $L_{2,3}$ XAS of the PCMO layer and a reference MnO bulk crystal that were measured concurrently in an upstream chamber. As the MnO ($Mn^{2+}$) spectrum differs from that of the PCMO layer and the signal of MnO of least energy is observed at 639 eV, it showed that PCMO is free of $Mn^{2+}$ ions. Further, a direct comparison with the Mn $L_{2,3}$ spectra reported earlier for PCMO and $La_{0.5}Sr_{0.5}MnO_3$ (**Fig. 2(b)**) showed a clear similarity between the spectrum of PCMO and those of well characterized bulk PCMO and $La_{0.5}Sr_{0.5}MnO_3$. The results thus confirmed that the PCMO thin film consisted of 50% $Mn^{3+}$and 50% $Mn^{4+}$ ions, as expected from the nominal stoichiometry.

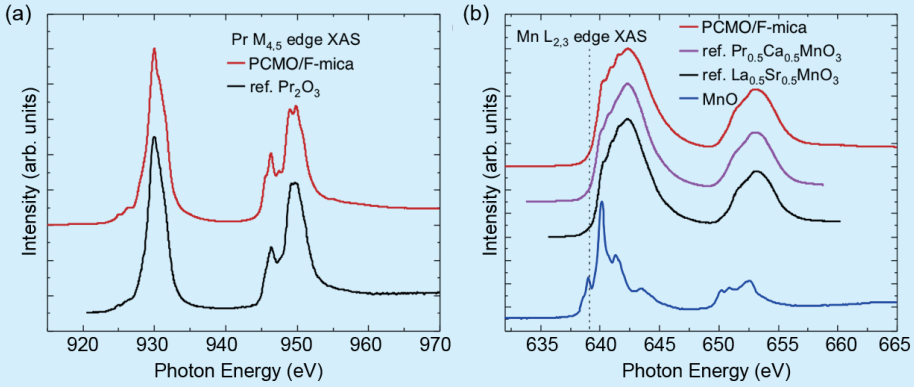


**Fig. 2**: X-ray absorption spectra of a) M-edge of Pr and b) L-edge of Mn of PCMO/STO on F-mica substrates. [Reproduced from Ref. 1]

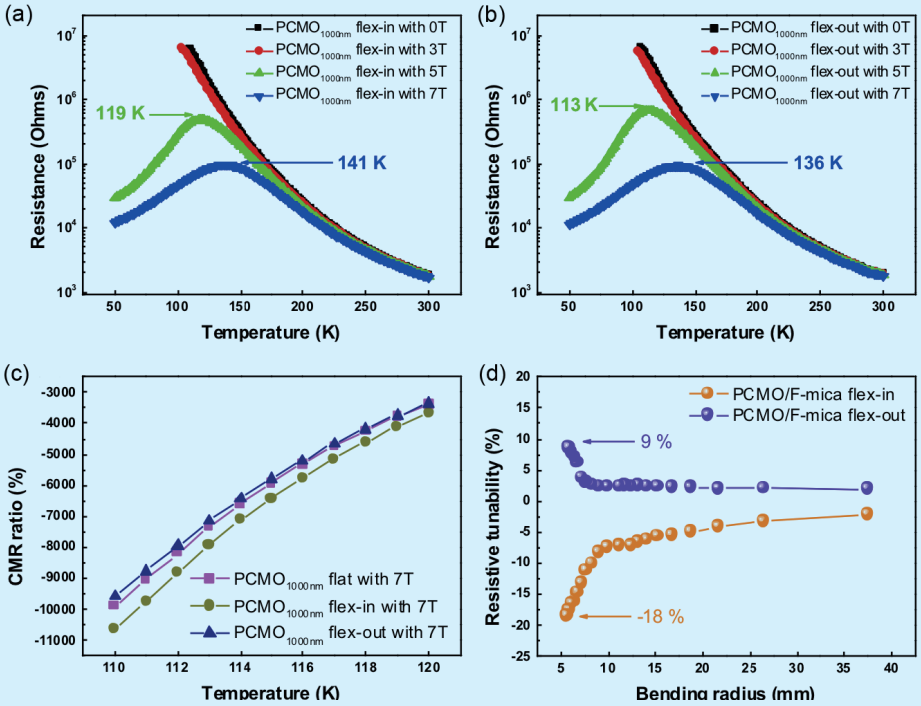


**Fig. 3**: Temperature-dependent resistance of a PCMO film on F-mica with (a) flex-in mode and (b) flex-out mode. (c) Temperature-dependent CMR ratios of a sample (thickness 1000 nm) with the flat, flex-in and flex-out modes. (d) Bending-radius-dependent resistive tunability at room temperature. [Reproduced from Ref. 1]

The authors also discussed the mechanical modulation of the transport properties as shown in **Figs. 3(a) and 3(b)**, which show the flex-in and flex-out mode magneto-transport measurements with bending radius 5 mm of inward/outward. On application of the two flexible modes, the melting fields in both cases appeared at magnetic field 5 T. Interestingly, the metal-insulator transition temperature $T_{MI}$ shifted upward in the flex-in mode and downward in the flex-out mode. The results clearly showed that the colossal magnetoresistance (CMR) properties of PCMO can be modulated by mechanical bending. **Figure 3(c)** shows a summary of the magneto-transport results. The authors observed a large bending-controlled modulation of the CMR ratio, $(R\text{-}R_0)/R \times 100\%$, achieving nearly 1000% at 110 K. Furthermore, to demonstrate a validity for practical applications, detailed bending tests were performed at room temperature, for which the data exhibited nearly 30% resistive tunability (**Fig. 3(d)**); the resistive tunability is calculated as $(R\text{-}R_0)/R_0 \times 100\%$. Cycling tests were also measured to show the endurance of PCMO/F/mica properties. The overall results showed excellent stability under both flex-in and flex-out modes at bending radius 5 mm for the PCMO/STO heteroepitaxial films grown on F-mica.[1] (Reported by Ashish Chainani)

*This report features the work of Ying-Hao Chu and his co-workers published in Adv. Funct. Mater.* ***30****, 2004597 (2020).*

## TLS 13A1 SW60 – X-ray Scattering

- XRD
- Materials Science, Condensed-matter Physics

## TLS 17B1 W200 – X-ray Scattering

- XRD
- Materials Science, Condensed-matter Physics

### TPS 45A Submicron Soft X-ray Spectroscopy

- XAS
- Materials Science, Condensed-matter Physics

### References


1. M. Yen, Y.-H. Lai, C.-Y. Kuo, C.-T. Chen, C.-F. Chang, Y.-H. Chu, Adv. Funct. Mater. **30**, 2004597 (2020).
2. Y. Bitla, C. Chen, H. C. Lee, T. H. Do, C. H. Ma, V. Q. Le, C. W. Huang, W. W. Wu, L. Chang, P. W. Chiu, Y. H. Chu, ACS Appl. Mater. Interfaces **8**, 32401 (2016).
3. S. Ke, J. Xie, C. Chen, P. Lin, X. Zeng, L. Shu, L. Fei, Y. Wang, M. Ye, D. Wang, Appl. Phys. Lett. **112**, 031905 (2018).
4. D. L. Ko, M. F. Tsai, J. W. Chen, P. W. Shao, Y. Z. Tan, J. J. Wang, S. Z. Ho, Y. H. Lai, Y. L. Chueh, Y. C. Chen, D. P. Tsai, L. Q. Chen, Y. H. Chu, Sci. Adv. **6**, eaaz3180 (2020).
5. J. Liu, Y. Feng, R. Tang, R. Zhao, J. Gao, D. Shi, H. Yang, Adv. Electron. Mater. **4**, 1700522 (2018).


# Skyrmions at Room Temperature

*The temperature range in which the skyrmion phase of $Cu_2OSeO_3$ is stabilized has been significantly enhanced from a small range, 55–58.5 K, to a large range, 5–300 K, on applying pressures up to 42.1 GPa.*

A skyrmion state is a special state observed in non-centrosymmetric helimagnets that exhibit topologically protected spin textures. The skyrmion state is considered promising for information technology, ultrarapid spintronics and microwave devices because an extremely small current is required to modify its spin configuration. To facilitate skyrmion applications, one great challenge is to expand the region of magnetic field–temperature phase space of the skyrmion state. Researchers have now found that the temperature region for the skyrmion phase in bulk $Cu_2OSeO_3$ can be greatly enhanced under applied physical pressure.[1]

The authors prepared single crystals of $Cu_2OSeO_3$; after characterizing the structure at ambient pressure, they measured $\chi'_{ac}(H)_{T,P}$ as a function of H at varied P up to 42.1 GPa and T up to 300 K, as shown in **Fig. 1**. The H–T regions in which the skyrmion state occurs at selected pressures, for example 2.5, 7.9, 26.2 and 42.1 GPa, are shown in **Figs. 1(a)–1(d)**, respectively. **Figure 1** clearly shows that the temperature region ($T_{A1}$,$T_{A2}$) for skyrmions (red shaded areas), or $\Delta T \equiv (T_{A2}-T_{A1})$, has been expanded from 55 K–58.5 K, that is, $\Delta T \sim 3.5$ K, at ambient pressures to 5 K–300 K), that is, $\Delta T > 290$ K, at 42.1 GPa by lowering $T_{A1}$ and raising $T_{A2}$ to above 300 K *via* pressure. The extension of $T_{A2}$ above 300 K above 7.9 GPa makes the skyrmion state accessible without the aid of liquid cryogen for device applications. At the same time, the field region ($H_{A1}$, $H_{A2}$) or $\Delta H \equiv$

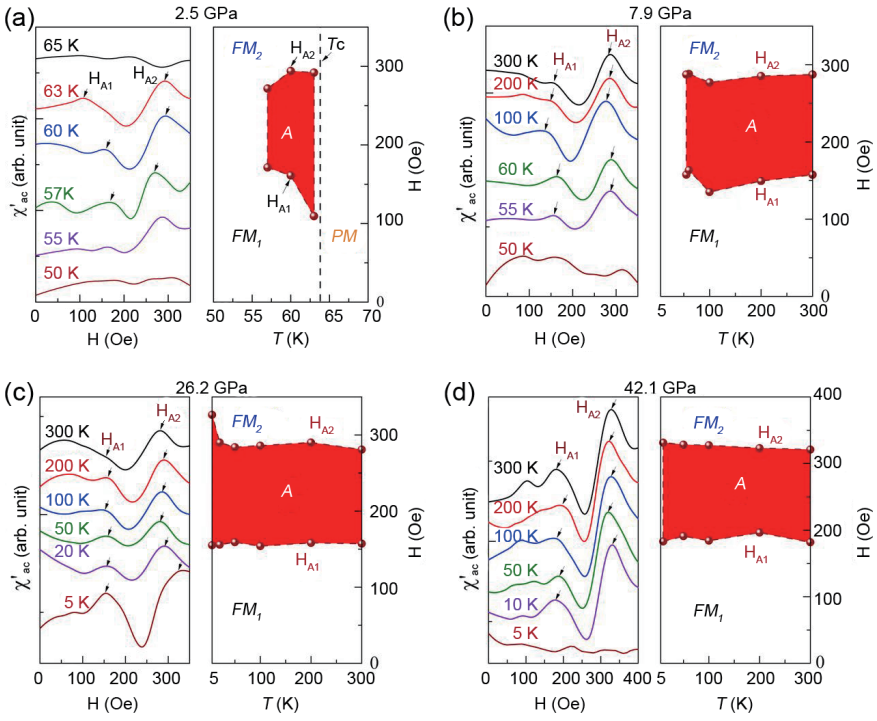


**Fig. 1**: ac susceptibility of $Cu_2OSeO_3$ as a function of magnetic field at varied critical pressures: (a) 2.5 GPa, (b) 7.9 GPa, (c) 26.2 GPa, (d) 42.1 GPa. The evolution of the "dip figure" indicates that the temperature region for the possible skyrmion state expands under pressure. At 7.9 GPa, the upper limit of the temperature range, $T_{A2}$, increases to 300 K, the highest temperature measured in this experiment. At 26.2 GPa, the lower limit of the temperature range, $T_{A1}$, extends to 5 K. With pressure increasing to 42.1 GPa, the "dip feature" becomes more pronounced while the temperature range remains between 5 to 10 K and 300 K. [Reproduced from Ref. 1]